

Diffusive vs Explosive Reaction at the Nanoscale

Snehaunshu Chowdhury, Kyle Sullivan, Nicholas Piekielek, Lei Zhou, and Michael R. Zachariah*

University of Maryland, College Park, Maryland 20742

Received: July 13, 2009; Revised Manuscript Received: October 11, 2009

Solid–solid reactions at the nanoscale between a metal passivated with a nascent oxide and another metal oxide can result in a very violent reaction. This begs the question as to what mechanism is responsible for such a rapid reaction. The ignition of nanoscale Al/CuO thermites with different aluminum oxide shell thicknesses were investigated on a fast heated ($\sim 10^5$ K/s) platinum wire. Ramping the wire temperature to ~ 1250 K and then shutting off the voltage pulse result in ignition well after the pulse is turned off; i.e., an ignition delay is observed. The delay is used as a probe to extract the effective diffusion coefficient of the diffusing species, which is confirmed by fast time-resolved mass spectrometry. The results of this study are consistent with a diffusion controlled ignition mechanism.

1. Introduction

Nanoscale particles composed of a metal and metal oxide can undergo a violent thermite reaction. Furthermore, it is well-known that making the particles smaller increases the reaction rate dramatically. An example of such a system is Al + CuO, which under stoichiometric conditions yields an adiabatic reaction temperature of 2840 K, with an energy density more than a factor of 3 over TNT on a volumetric basis. Nevertheless, because of the interrelationship between many complex processes occurring, considerable debate continues as to the nature of initiation of the thermite event. Close proximity of the fuel and oxidizer reduces the diffusion length and increases the reaction rate.¹ Fuel nanoparticles usually have a lower melting point than their micrometer size counterparts,^{2,3} making them easier to ignite. However, for very small particles, heat transfer rates are extremely fast and hence reaction characteristics such as the onset of reaction, ignition temperature, ignition delays, etc. are known to depend on the particle size.^{4–6}

We consider the Al/CuO nanoscale thermite system as representative of the wide class of such reactions. The aluminum fuel component is actually a core shell structure of an aluminum core with an aluminum oxide passivation layer. Typically, such layers are on the order of a few nanometers.⁷ The interaction between the low melting core and high melting shell is critical in understanding the ignition mechanism at the nanoscale. Nominally, we consider the nanoscale regime to be those where both components (metal and metal oxide) are below 100 nm in diameter.

It is important, before proceeding further, to define some terminologies. Ignition temperature is defined as the temperature at which a particle/mixture can sustain chemical reaction on its own, without the aid of an external heat source. The ignition temperature is a strong function of experimental conditions as well as material property.

Several researchers have reported that the ignition temperature of micrometer sized aluminum is very close to the melting point of the metal oxide (Al₂O₃) shell.^{8–14} On the other hand, nanosized aluminum exhibits much lower ignition temperatures closer to the melting point of aluminum.^{15–19} In other cases

reaction (but not ignition) occurs at well below the melting point when probed by low heating rate experiments (tens of K/min). For example, Umbrajkar et al.¹⁶ reports evidence of reaction occurring at temperatures as low as 400 K in thermal analysis experiments. However, the reaction rate in such systems is not high enough to lead to thermal runaway and ignition. In shock tubes with heating rates of $\sim 10^6$ K/s the ignition temperature of nanoaluminum has been observed to be in the range 1200–2100 K at elevated pressures.¹³ Nanoaluminum, thus, has been reported to have a wide range of ignition temperatures as compared to micrometer sized aluminum. Studies also report the effect of the type of shell and its thickness on the chemical reactivity of the particle. Jones et al.²⁰ found that aluminum nanoparticles with aluminum oxide and Teflon coatings have remarkable differences in their reactivity toward water. Levitas et al.²¹ has suggested that an initiation event via the melt dispersion mechanism (described below) would be promoted if the temperature of formation of the oxide shell is increased.

Two different mechanisms have been proposed in the literature to explain the observed behavior for nanoaluminum. These mechanisms differ significantly in the way ignition occurs. The first mechanism states that the ignition and reaction of nanoaluminum has a diffusion based mechanism where participating species diffuse across the oxide shell. Rai et al.²² has shown that even with a low heating rate, the aluminum core melts and exerts pressure on the oxide shell, causing it to crack (not violently). In contrast, the melt dispersion mechanism, proposed by Levitas et al.,²¹ requires the mechanical rupture of the shell and thereby release of the aluminum for ignition/reaction. According to this mechanism, under high heating rates the core melts very quickly and volumetrically expands while the oxide shell remains solid. If the stress on the shell becomes high enough, it causes the oxide shell to suddenly rupture explosively followed by the ejection of small molten aluminum clusters.²¹ However, the current knowledge about the exact physical mechanism is still unclear.

A resolution of the two opposing views is the subject of this article. The assessment of the prevailing mechanism is done by systematically changing the thickness of the oxide shell to determine the ignition temperature and characteristic reaction time. Our studies will show that this highly violent reaction is likely based on a diffusion mechanism.

* Corresponding author. Phone: 301-405-4311. Fax: 301-314-9477. E-mail: mrz@umd.edu.

TABLE 1: Preparation of Aluminum for 3 Al/CuO Stoichiometric Mixtures

sample	time in preheated furnace at 500 °C (min)	shell thickness calculated from weight gain (nm)	activity (%)
1		2	70
2	5	3	59
3	10	4	50

2. Experiment

In this study we prepare mixtures of Al/CuO nanoparticles that are coated onto a fine wire. The wire is rapidly joule heated using a preprogrammed voltage pulse and the point of ignition is recorded with a photomultiplier tube. In addition, time-resolved time-of-flight mass-spectrometry enables us to obtain temporal speciation of the reaction. The key point is the preparation of metal with different oxide thicknesses, and our ability to accurately measure temperature during heating rates of $\sim 10^5$ K/s.

(a) Sample Preparation. Commercially available aluminum powder ALEX procured from Argonide Corp. has been used in this study. The particles have a nominal size of ~ 50 nm with an active aluminum content of $\sim 70\%$ determined by thermogravimetric analysis (TGA). This would indicate an aluminum oxide shell thickness of ~ 2 nm, which is consistent with TEM analysis. To increase the oxide thickness, particles were oxidized at 500 °C (i.e., below the melting point of aluminum) for various lengths of time and subsequently weighed to determine the oxide growth. This ensures that the oxide shell thicknesses are formed at the same temperature, an important criterion in the melt dispersion mechanism. The shell thickness is calculated on the basis of the weight gain and assuming spherical particles and bulk densities for Al and Al_2O_3 . The process was repeated until the gain in weight corresponded to thickening of the oxide shell to ~ 3 and 4 nm. The active aluminum content in those samples is thus changed to 59 and 50%, respectively. These measurements have an accuracy of $\pm 3\%$ limited by precision of the balance (0.1 mg). An appropriate amount of copper(II) oxide nanopowders (< 100 nm size) from Sigma Aldrich is weighed and mixed with the aluminum powders with different shell thicknesses to make three stoichiometric mixtures. Hexane is then added to the samples and sonicated for ~ 30 min to intimately mix the fuel and oxidizer. Table 1 shows the preparation and composition of aluminum in the three samples.

(b) Experimental Setup. A thin platinum wire (length ~ 12 mm, diameter ~ 76 μm) is joule heated by a tunable voltage pulse generated by a home-built power source. For any applied voltage (i.e., heating rate) the temperature to which the wire is heated can be controlled by varying the duration of the pulse, and the current passing through the circuit is measured transiently by a current probe. A small portion of the central region of the wire (~ 3 – 4 mm) is coated with the samples using a micropipette and the hexane is allowed to evaporate, leaving a dense coating on the wire. The ignition event is recorded using a photomultiplier tube (PMT) and is identified by the appearance of a sudden emission of light above the background signal from the heated wire. In the context of this paper, ignition delay is defined as the time difference between the appearance of the ignition signal, identified as a sharp spike in the optical detector, and the end of the applied voltage pulse.

From the recorded voltage and current data, the temperature of the wire at the point of ignition can be calculated from the well-known Callender–Van Dusen equation.²³ A new wire is used each time a sample is heated.

3. Results

Figure 1a shows the temperature of the wire and the PMT signal recorded as a function of time for such an event, for the three samples in Table 1 under condition of a heating rate of 1.7×10^5 K/s. Heating rates were fairly repeatable with uncertainty $\sim 10^4$ K/s. The uncertainty associated with the measurement of maximum temperature is ± 50 K, based on several factors including contact resistance, length of wire, etc. The sharp rise in the PMT signal indicates the start of the reaction. The results show an apparent increase in ignition temperature from 1275 to 1450 K as the shell thickness is increased. Please note that in this case, the wire temperature is being ramped past the ignition temperature. In a second experiment we vary the heating rate (1.7×10^5 and 5.2×10^5 K/s) and plot the result in Figure 1b for a particle with a 2 nm shell. Clearly observed is that the ignition temperature is heating rate independent in the range of heating rates carried out in this study. Similar behavior is observed for samples 2 and 3. The maximum heating rate is limited by the power supply and the shortest pulse duration that would not melt the platinum wire.

A next set of experiments are conducted in which we shut off the voltage pulse at a temperature below where the optical emission was observed in Figure 1a. What we observed was that the powders could still be ignited even after the pulse had been shut off; *there is a very clear delay associated with ignition*. We define the ignition delay as the time difference between when the pulse is shut off and the onset of optical emission. The maximum temperature of the wire is 1250 K in all runs and was decided by iteratively lowering the maximum temperature until just before no ignition was seen. Therefore, we are only heating the particles just to their ignition temperature and then observing as the ignition subsequently occurs.

The experimental data for the three different oxide shell thicknesses are shown in Figure 2. In all three samples, the wire was heated to 1250 K at 3.2×10^5 K/s and then shut off. This temperature is just around the lowest ignition temperature of any particle determined in Figure 1a. The ignition delays were fairly repeatable, with samples 1 (~ 20 μs) and 2 (~ 50 μs) showing lesser variability than sample 3 (~ 100 μs). Since the heating pulses for the three samples are the same, in the absence of any reaction the system would be cooling. Despite this, a reaction event occurs, and the event time correlates with oxide shell thickness. *This is the key result of this paper which we will interpret.*

Finally, time-resolved time-of-flight mass spectrometry of Al–CuO nanothermites is also conducted on the samples as a qualitative tool to verify the delay in ignition. A description of the instrument, its operating procedures, and verification could be found elsewhere.²⁴ Figure 3 shows time-resolved mass spectra taken at 100 μs intervals for sample 1, the 2 nm shell thickness case. Species with strong signals, such as H_2O^+ ($m/z = 18$) and N_2^+ ($m/z = 28$) are background species while HCHO^+ ($m/z = 30$) and CO_2^+ ($m/z = 44$) appears from the small amount of copper carbonate formed on the surface of CuO. In this experiment, the heating pulse was turned off around 2.35 ms. Very relevant is that no Al^+ ($m/z = 27$) is seen before 2.35 ms but appears at ~ 2.4 ms. Cu^+ ($m/z = 63.0$) starts appearing at ~ 2.5 ms, suggesting an ignition delay of ~ 150 μs . This compares very closely to the optical measurement, which has better time resolution. Cu is never observed when CuO alone is heated and its appearance in mass spectrometry is analogous to the sharp rise in the PMT signal, as Cu is present only as a product species and indicates the start of the reaction. O_2^+ ($m/z = 32$) appears from the decomposition of CuO, $2\text{CuO} \rightarrow \text{Cu}_2\text{O}$

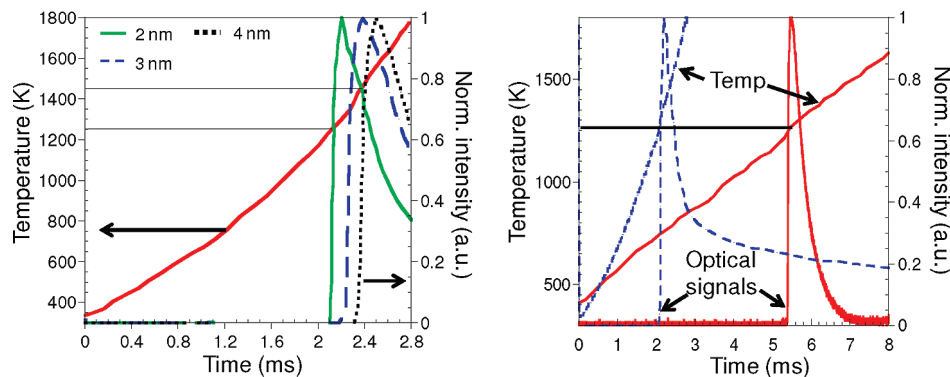


Figure 1. (a) Ignition temperature for samples 1, 2, and 3 at 5.3×10^5 K/s. (b) Effect of heating rate [1.7×10^5 K/s (blue) and 5.2×10^5 K/s (red)] on ignition temperature of sample 1.

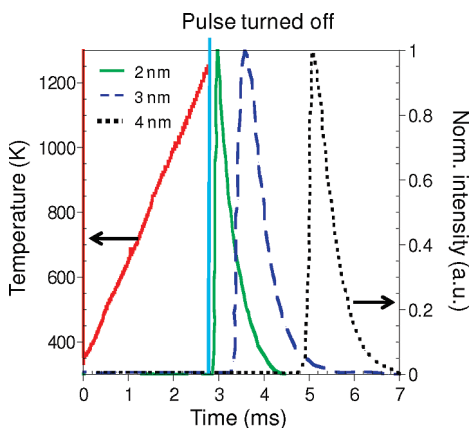


Figure 2. Ignition delay as observed with samples having different oxide shell thicknesses on aluminum. The maximum temperature attained by the wire is 1250 K, as indicated by the red curve. The wire cools down ~ 50 K in the longest times scales seen here after the pulse is turned off. Heating rate is $\sim 3.2 \times 10^5$ K/s.

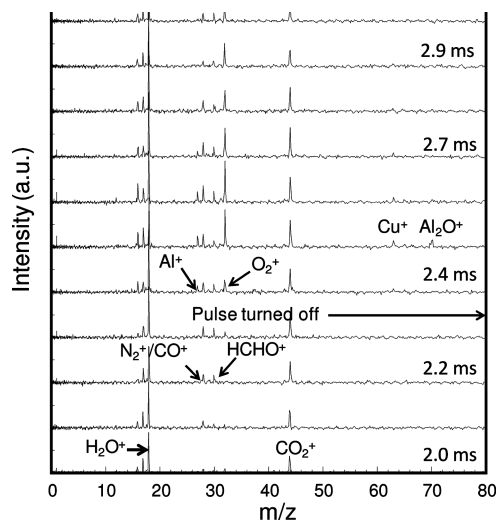


Figure 3. Time of flight mass spectrometric measurements for sample 1. The temperature of the wire when the pulse is turned off is around 1300 K. The species mentioned before the pulse is turned off emanates from background.²⁵

+ $1/2$ O₂ and is seen before the pulse is turned off. Cu always appears in the same or after one spectrum of the appearance of Al. Another product species Al₂O⁺ ($m/z = 70$) appears around the same time as copper. A more detailed description of the mass spectrometric measurements on Al–CuO thermites is available in Zhou et al.²⁵ Similar results were seen for samples

2 and 3, except that copper seemed to appear even later in the spectrum with increase in shell thickness.

4. Discussion

The independence of ignition temperature on heating rate for any given shell thickness is possibly a first suggestion against the melt dispersion mechanism, as it is expected to be very sensitive to heating rate. However, the range of heating rates is fairly small in our case, which is restricted by the power supply. The change in ignition temperature in Figure 1a with oxide thickness could be explained as due to a longer path to diffuse through the oxide shell, rather than an increase in temperature. This point is most reinforced by the key observation in this work (Figure 2), that ignition occurs after the pulse is turned off, and thus energy input to the system has ceased. Furthermore, the thicker the oxide shell, the greater the ignition delay—again consistent with a diffusion mechanism. According to the melt dispersion mechanism, reaction would occur at the melting point of aluminum owing to the maximum mismatch in thermal expansion coefficient between the molten aluminum core and the solid oxide shell.

A simplified simulation based on the model developed by Ward et al.²⁶ was carried out to estimate the actual powder temperature. Results show that the powder temperature is < 5 K from the wire temperature. Also, once the pulse is shut off, the heat loss from the wire due to convection and radiation is minimal, which over the relevant time of the experiment decreases no more than ~ 50 K. This would indicate the ignition temperature of the powder exceeds the melting point of aluminum (~ 933 K) and contrary to what is expected according to the melt dispersion mechanism. The characteristic heat transfer time across a nanoparticle is on the order of a few nanoseconds, so that melting should occur essentially instantaneously once the melting point is exceeded. This would cause a huge buildup in internal pressure, and hence explode violently, in time scales on the order of nanoseconds. However, we see no evidence of reactions at such time scales; rather we see delay times of ~ 100 s of microseconds.

The melt dispersion mechanism is expected to happen at very high heating rates of 10^6 – 10^8 K/s.²⁷ This was phenomenologically suggested from the rise time observed in pressure traces in burn tube experiments.¹ However, in those experiments, the powder was set off by an electrical igniter. The external heating rate is thus unknown, and hence, the above-mentioned rate is clearly the “intrinsic” heating rate once the powder has ignited. The adiabatic flame temperature of the Al–CuO mixture is ~ 2840 K, and the ignition temperature seen in this study is ~ 1200 K. The rise time (time for the optical signal to go from

TABLE 2: Ignition Delay and Effective Diffusion Coefficient with Oxide Shell Thickness

oxide shell thickness, L (nm)	t_{delay} (μs)	D_{eff} (cm^2/s)
2	100	4.0×10^{-10}
3	500	1.8×10^{-10}
4	2000	8.0×10^{-11}

0 to 1 in Figure 2) observed in the optical signal is $\sim 100 \mu\text{s}$. This would suggest an intrinsic heating rate of $\sim 1.6 \times 10^7 \text{ K/s}$, which is within the range of the melt dispersion mechanism. As a result, we would assume that the “intrinsic” heating rate of the powder was sufficient to observe the melt dispersion mechanism if it were to happen.

An order of magnitude estimate of the effective diffusion coefficient ($=L^2/t_{\text{delay}}$) is presented in Table 2, with the delay times reported as an average of two experiments and the characteristic diffusion length (L) assumed to be the thickness of the shell. The extracted diffusion coefficients, assuming a transport controlled mechanism seem quite reasonable.²⁸

The appearance of Cu^+ signal in mass spectrometry follows the same trend that we see in our optical experiments. We use Cu as evidence of reaction since it does not appear when we heat pure CuO, but rather only when the aluminum is present. Cu gas is a major reaction product of stoichiometric Al/CuO under vacuum, and so its signature is a strong indicator that the reaction is occurring. The appearance of copper later in the spectrum for samples 2 and 3 (relative to sample 1) indicates a delay in the initiation of those reactions and supports the diffusion controlled mechanism.

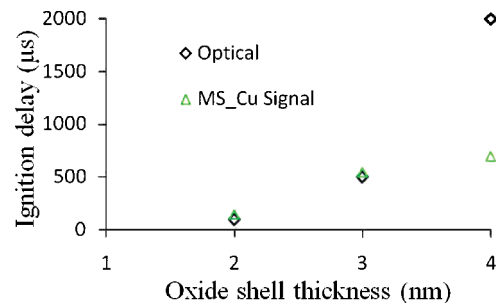
On the basis of the ignition temperature, the aluminum core would be molten. Although the purpose of this paper is not to determine the diffusion species, it is the aluminum ions from the molten core that are more likely to diffuse because of their smaller size relative to oxygen ions. Evidence of the dominance of the diffusion of aluminum has been observed in other studies too. Rai et al.²⁸ have shown the formation of hollow particles during aluminum oxidation where the molten aluminum in the core has leaked out and reacted. Similar hollow particle formation has also been reported by Nakamura et al.²⁹ Henz et al.³⁰ has also recently showed that intrinsic electric fields within the nanoparticle promote the movement of aluminum ions through the oxide shell, which significantly enhance the initial transport over Fickian diffusion.

Once the reaction starts, an increase in temperature will cause enhancement in diffusion of all diffusing species. Although, on the basis of references 28 and 29, we would expect all the aluminum in the core to leak out faster, we do not have direct evidence of this and cannot from this set of experiments conclude more on the nature of the diffusing species.

Finally, in Figure 4 we summarize the ignition delay observed for the various cases tested. Ignition delay increases with an increase in shell thickness, with the 4 nm shell showing the longest delay. The mass spectrometric data compare well qualitatively with the optical data and shows the same trend as identified by the appearance of the Cu signal. These observations point to an initiation mechanism governed by diffusion across the oxide shell.

5. Conclusions

Experiments were conducted at high heating rates to investigate the ignition mechanism of nanothermites. Aluminum nanoparticles were prepared with varying oxide shell thicknesses and were mixed with CuO to investigate the ignition behavior

**Figure 4.** Ignition delay time as a function of various oxide shell thicknesses.

at high heating rates of $\sim 10^5 \text{ K/s}$. We find the ignition temperature is well above the melting point of aluminum, and ignition was not observed below 1250 K. Furthermore *an ignition delay consistent with a diffusion limited reaction is observed*. The delay increased with an increase in shell thickness of aluminum particles in the samples, and from this, effective diffusion coefficients were extracted. Fast time-of-flight mass spectrometry shows that the appearance of copper, which is a product species, is progressively delayed in the mass spectra with an increase in the shell thickness and agrees with the order of ignition delay observed. On the basis of our data, we would conclude that ignition under the heating rates investigated has a *diffusion governed mechanism*.

Acknowledgment. Support for this work has been provided by the Defense Threat Reduction Agency (DTRA) and the Army Research Office (ARO).

References and Notes

- (1) Bockmon, B. S.; Pantoya, M. L.; Son, S. F.; Asay, B. W.; Mang, J. T. *J. Appl. Phys.* **2005**, *98*, 064903.
- (2) Puri, P.; Yang, V. *J. Phys. Chem. C* **2007**, *111*.
- (3) Alavi, S.; Thompson, D. L. *J. Phys. Chem. A* **2006**, *110*, 1518.
- (4) Moore, K.; Pantoya, M. L. *J. Prop. Power* **2007**, *23*, 1.
- (5) Sun, J.; Pantoya, M. L.; Simon, S. L. *Thermochim. Acta* **2006**, *444*, 117–127.
- (6) Bulian, C. J.; Kerr, T. T.; Puszynski, J. A. *31st International Pyrotechnics Seminar, Fort Collins, CO, July 12–14, 2004*; International Pyrotechnics Seminar U.S.A., Inc.: Marshall, TX, 2004; p 327.
- (7) Wilson, D. E.; Kim, K. 30th AIAA/ASME/SAE/ASEE Joint Prop. Conf., 2003, Reno, Nevada.
- (8) Dreizin, E. L. *Combust. Flame* **1996**, *105*, 541–546.
- (9) Friedman, R.; Macek, A. *Combust. Flame* **1962**, *6*, 9.
- (10) Merzhanov, A. G.; Grigoriev, Y. M.; Galchenko, Y. A. *Combust. Flame* **1977**, *29*, 1.
- (11) Trunov, M. A.; Schoenitz, M.; Zhu, X.; Dreizin, E. L. *Combust. Flame* **2005**, *140*, 310.
- (12) Trunov, M. A.; Schoenitz, M.; Dreizin, E. L. *Joint Meeting of the U.S. Sections of The Combustion Institute, Philadelphia, PA*; The Combustion Institute: Pittsburgh, PA, 2005.
- (13) Bazyn, T.; Krier, H.; Glumac, N. *Combust. Flame* **2006**, *145*, 703–714.
- (14) Bazyn, T.; Glumac, N.; Krier, H.; Ward, T. S.; Schoenitz, M.; Dreizin, E. L. *Combust. Sci. Technol.* **2007**, *179*, 457–476.
- (15) Aumann, C. E.; Skofronick, G. L.; Martin, J. A. *J. Vac. Sci. Technol. B* **1995**, *13* (3), 1178–1183.
- (16) Umbrajkar, S. M.; Schoenitz, M.; Dreizin, E. L. *Thermochim. Acta* **2006**, *451*, 34–43.
- (17) Pantoya, M. L.; Granier, J. J. *J. Thermal Anal. Calorim.* **2006**, *85* (1), 37–43.
- (18) Park, K.; Lee, D.; Rai, A.; Mukherjee, D.; Zachariah, M. R. *J. Phys. Chem B* **2005**, *109*, 7290.
- (19) Trunov, M. A.; Schoenitz, M.; Dreizin, E. L. *Propellants, Explosives, Pyrotechnics* **2005**, *30* (1), 36–43.
- (20) Jones, D. E. G.; Turcotte, R.; Fouchard, R. C.; Kwok, Q. S. M.; Turcotte, A. M.; Qader, Z. A. *Propellants Explosives Pyrotech.* **2003**, *28*, 120–131.
- (21) Levitas, V. L.; Asay, B. W.; Son, S. F.; Pantoya, M. L. *Appl. Phys. Lett.* **2006**, *89*, 071909.

(22) Rai, A.; Lee, D.; Park, K.; Zachariah, M. R. *J. Phys. Chem. B* **2004**, *108* (39), 14793.

(23) Childs, P. R. N. *Practical Temperature Measurement*; Butterworth-Heinemann: London, 2001; Chapter 6, p 149.

(24) Zhou, L.; Piekiet, N.; Chowdhury, S.; Zachariah, M. R. *Rapid Commun. Mass Spectrom.* **2009**, *23*, 194–202.

(25) Zhou, L.; Piekiet, N.; Chowdhury, S.; Zachariah, M. R. Manuscript in preparation.

(26) Ward, T. S.; Trunov, M. A.; Schoenitz, M.; Dreizin, E. L. *Intl. J. Heat Mass Transfer* **2006**, *49*, 4943–4954.

(27) Levitas, V. I.; Pantoya, M. L.; Watson, K. W. *Appl. Phys. Lett.* **2008**, *92*, 201917.

(28) Rai, A.; Park, K.; Zhou, L.; Zachariah, M. R. *Combust. Theory Modell.* **2006**, *10*, 843–859.

(29) Nakamura, R.; Tokozakura, D.; Nakajima, H.; Lee, J. G.; Mori, H. *J. Appl. Phys.* **2007**, *101*, 074303.

(30) Henz, B.; Hawa, T.; Zachariah, M. R. *J. Appl. Phys.*, in press.

JP906613P